

19. Jones JG, Royston D, Minty BD. Changes in alveolar-capillary barrier function in animals and humans. *Am Rev Respir Dis* 1983;127:S51-S59.
20. Dusser DJ, Minty BD, Collignon MG, Hinge D, Barritault LG, Huchon GJ. Regional respiratory clearance of aerosolized ^{99m}Tc-DTPA: posture and smoking effects. *J Appl Physiol* 1986;60:2000-2006.
21. Smith RJ, Hyde RW, Waldman DL, et al. Effect of pattern of aerosol inhalation on clearance of technetium-99m-labeled diethylenetriamine pentaacetic acid from the lungs of normal humans. *Am Rev Respir Dis* 1992;145:1109-1116.
22. Groth S, Hermansen F, Rossing N. Pulmonary permeability in never-smokers between 21 and 67 yr of age. *J Appl Physiol* 1989;67:422-428.
23. Child CG III, Turcotte CG. Surgery and portal hypertension. In: Child CG III, ed. *The liver and portal hypertension*. Philadelphia: WB Saunders; 1964:50.
24. Spagnolo SV. Cyanosis of cirrhosis. *Med Clin North Am* 1975;59:983-987.
25. Berthelot P, Walker JG, Sherlock S, Reid L. Arterial changes in the lungs in cirrhosis of the liver—lung spider nevi. *N Engl J Med* 1966;274:291-298.
26. Ohara N, Voelkel NF, Chang SW. Tissue eicosanoids and vascular permeability in rats with chronic biliary obstruction. *Hepatology* 1993;18:111-118.
27. Chang SW, Ohara N. Increased pulmonary vascular permeability in rats with biliary cirrhosis: role of thromboxane A₂. *Am J Physiol* 1993;264:L245-L252.
28. Kuroyanagi T, Kura K. A new method for evaluating an increased general capillary permeability in patients. *Tohoku J Exp Med* 1977;122:331-336.
29. Guyton AC. Physical principles of gaseous exchange; diffusion of oxygen and carbon dioxide through the respiratory membrane. In: Guyton AC, ed. *Textbook of medical physiology*, 8th ed. Philadelphia: W.B. Saunders; 1991:422-432.
30. West JB. Uptake and delivery of the respiratory gases. In: West JB, ed. *Best and Taylor's physiological basis of medical practice*, 11th ed. Baltimore: Williams & Wilkins; 1985:546-571.
31. Mines AH. Gas exchange in the lungs. In: Mines AH, ed. *Respiratory physiology*, 2nd ed. New York: Raven Press; 1986:103-128.
32. Rizk N, Luce J, Hoeffel J, et al. Site of deposition and factors affecting clearance of aerosolized solute from canine lungs. *J Appl Physiol* 1984;56:723-729.
33. Braude S, Royston D, Coe C, Barnes P. Histamine increases lung permeability by an H₂-receptor mechanism. *Lancet* 1984;18:372-374.
34. Alekseevskikh IUG. State of the air-blood barrier in experimental liver cirrhosis. *Arkh Patol* 1982;44:36-42.

Whole-Body PET: Physiological and Artifactual Fluorodeoxyglucose Accumulations

Hermann Engel, Hans Steinert, Alfred Buck, Thomas Berthold, Rahel A. Huch Böni and Gustav K. von Schulthess
 Divisions of Nuclear Medicine and Diagnostic Radiology, Department of Medical Radiology, University Hospital, Zürich, Switzerland

The purpose of this study was to semiquantitatively identify artifactual and physiological soft-tissue accumulations in whole-body FDG-PET scans with the aim of defining their frequency and anatomic distribution. **Methods:** Fifty whole-body FDG-PET scans performed for the staging of malignant melanoma were obtained from transaxial scans and reconstructed without absorption correction by filtered backprojection in the form of coronal and sagittal sections. The patients were asked to stay n.p.o. for at least 4 hr and interrogated about their physical activity prior to injection and until scanning. Classification of FDG organ accumulations was done using grades 0-6. Means and standard deviations on this scale were then calculated for multiple organs and muscle groups and tabulated. **Results:** On this grading scale, viscera showed uptake grades between 1.7 ± 0.5 and 2.05 ± 1.0 . Except for the intestines, the activity in these organs was homogeneously distributed. Relatively high average uptake values of 2.0-4.2 (s.d. ≥ 2.3) were found in various muscle groups, especially the orbital musculature. Myocardial uptake was visible in 90% of the scans. Reconstruction artifacts were seen around the renal collecting system and the bladder. **Conclusion:** Most of the "normal" accumulations of FDG in nonattenuation corrected whole-body PET are readily recognized and distinct from the usually focal FDG accumulation associated with metastatic disease, but the diagnostician must be familiar with them. Muscular FDG uptake is related to physical activity prior and immediately following injection and can be minimized by proper patient instructions and positioning.

Key Words: PET; fluorine-18-FDG; physiological accumulations

J Nucl Med 1996; 37:441-446

With the introduction of PET scanners with high detection efficiency and a large axial field of view of 15 cm or more, whole-body PET with [¹⁸F]fluorodeoxyglucose (FDG) has become a clinical reality. Typically, axial scan distances of 150 cm

can be covered in 60 min (two-dimensional mode) and substantial improvement in acquisition time can be expected from the introduction of three-dimensional data acquisition protocols. The result of such whole-body data acquisition is a set of 450 or more transaxial slices that can be reformatted into coronal and sagittal planes at will (Fig. 1). Several studies have documented PET as a sensitive method for tumor staging because FDG preferentially accumulates in many types of malignant tumor cells (1-8) and has well recognized physiological accumulation sites (4,5,9-12).

When reading whole-body PET scans, it is important to distinguish physiological and artifactual FDG accumulations from those that are pathological (1,4), as normal findings have to be distinguished from those that are abnormal in any imaging method. In this study, we analyzed the occurrence and appearance of such "normal" activity accumulations in nonattenuation-corrected whole-body FDG-PET scans by looking at a multitude of organ sites.

MATERIALS AND METHODS

Patients

Fifty whole-body PET scans were obtained in patients referred for tumor staging of malignant melanoma. The patients (30 men, 20 women) ranged in age from 18 to 80 yr. Patients with diabetes mellitus were excluded because of their pathologic glucose metabolism which affects FDG uptake in an uncontrolled fashion unless glucose clamping is used (13). All patients participating in this study consented to having a PET scan. Each patient was questioned about their physical activities in the period preceding FDG injection and whether they had been comfortable during the phase between injection and scanning and the PET examination itself.

PET

The patients were explicitly asked to stay n.p.o. for at least 4 hr prior to the study. Thirty to 40 min prior to scanning, the patients received an intravenous injection of 220-370 MBq [¹⁸F]FDG while lying on a stretcher in a silent room. FDG was produced at the Paul Scherrer Institute (Villigen, Switzerland) using well

Received Jan. 24, 1995; revision accepted Jun. 29, 1995.

For correspondence or reprints contact: Gustav K. von Schulthess, MD, PhD, Division of Nuclear Medicine, Department of Medical Radiology, University Hospital, CH-8091 Zürich, Switzerland.



FIGURE 1. Standard whole-body PET images show normal distribution of accumulation in (left) coronal and (right) sagittal sections. Note strong activity in the brain, the renal pelvis and the bladder, all giving rise to a reconstruction artifact. Distinct activity is noted in the skin, lungs, liver and the renal parenchyma, as well as in the vertebral bodies. No activity is present in regions of cortical compact bone such as the femora and vertebral plates, including the disks. In the coronal scan, spot-like ureteral activity is noted at the level of the sacro-iliac joint. Activity in the left lower thorax is in the posterior myocardial wall.

known techniques (14). During the time between injection and scanning, the patients were asked to remain still to keep physiological FDG consumption of the striated muscle on a low level. Since FDG follows the first step of cellular glucose metabolism, we would expect increased FDG accumulation in activated striated muscle. Of the 50 patients, 24 had a scan covering the body area from the head to the bottom of the pelvis, while 26 had scans covering the entire body, including the lower extremities. PET scanning was done using a GE Signa Advance PET Scanner (GE Medical Systems, Milwaukee, WI) in the whole-body mode. Once the measurement was accomplished, the table position was incremented by 14.6 cm and the acquisition process started anew. Up to 13 increments could be preprogrammed so that a total axial field of view up to 180 cm could be obtained in approximately 65 min.

To minimize image degradation from the bladder region, due to

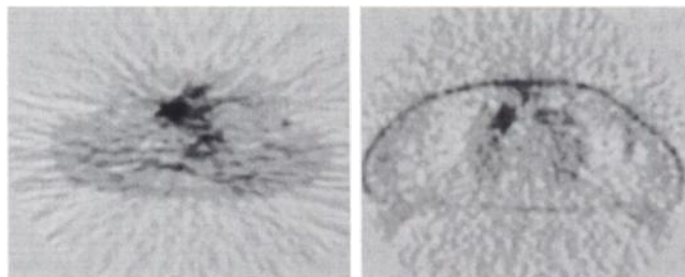


FIGURE 2. Comparison of thorax scans with (left) attenuation correction and (right) without attenuation correction.

renal excretion of FDG, all patients were asked to void just prior to scanning. With a minimum amount of activity in the bladder, scanning was begun in the pelvic region and then proceeded towards the patient's head. In cases where the lower extremities were also to be scanned, this region was scanned subsequently. The acquired data were reconstructed into transaxial slices using standard filtered backprojection techniques from which coronal and sagittal views were obtained.

No attempt was made to correct for attenuation by acquiring transmission scans for two reasons:

1. Imaging time would have been at least doubled, resulting in extremely long acquisition times, which is unacceptable for clinical purposes.
2. Attenuation correction using a relatively short data acquisition time of 5 min produced noisy reconstructed images, often resulting in inadequate image quality (Fig. 2).

All images were documented using a standard color laser copier [retrofitted with a special digital interface] after appropriate windowing and leveling. The window and level setting were determined so that FDG accumulation on the upper end of the intensity scale (i.e., in the brain) appeared very intense but enough contrast was still present to distinguish the cerebral sulci on the coronal and sagittal images. On the lower end of the intensity scale, the window and level setting were chosen so that the patient's body surface was still clearly visible and the background still within the lowest range of the window. The relative constancy of brain FDG accumulation (9,10) determined that scans were visually comparable regarding activity distribution patterns.

Data Analysis

Our data analysis scheme was practical and useful when evaluating clinical whole-body PET examinations. The windowing and leveling process was done as previously described. On the basis of extensive deliberations among four observers over five whole-body scans, a grading scheme of 0–6 was introduced. This scheme assigned the value 5 to brain activity and 1 to background activity in each patient. With this scale, bladder activity typically showed such high accumulation, that with the windowing and leveling scheme used, the activity was in an “over-range” to which grade 6 was assigned. Thirty-seven organs and muscle groups were then classified according to the 0–6 grading scale (Table 1). For important organs and some selected muscle groups, mean and standard deviation of grades were subsequently calculated.

Whenever activity accumulation that could not clearly be classified as physiological or artifactual was observed, analysis of other cross-sectional imaging data was used to ascertain no correlation to a pathological process. The presence of suspicious pathological processes was ascertained bioptically or by other cross-sectional imaging modalities.

TABLE 1
Means and s.d. for Semiquantitative Activity

Organ/Muscle	s.d.	Mean
Brain	0	5
Background	0	1
Skin	0.28	2.09
Oral cavity	1.06	2.72
Breast	0.7	1.23
Lung	0.5	1.91
Myocardium	1.78	2.61
Liver	0.56	2.05
Intestine	1	1.7
Kidneys	0.7	1.94
Ureter	0.96	0.31
Sternocleidomastoid	1.66	2.03
Medial forearm	0.7	2.2
Lateral forearm	1.1	3.28
Vastus lateral	1.27	1.54
Peroneus longus	2.35	2.92
Gastrocnemius	1.56	2.31
Ocular muscles	1.1	4.21

RESULTS

As expected, substantial physiological accumulation was seen in the brain (Fig. 1). Since glucose consumption of the brain is relatively constant, brain activity serves as a good qualitative activity reference site. The heart can also accumulate FDG in patients who have been fasting prior to scanning (11,12). Although patients were asked not to drink or eat during the 4 hr prior to scanning, 17 of 50 patients showed myocardial activity ≥ 4 . Homogeneous activity with a grade of around 2 was noted in the lungs and never exceeded grade 3. The liver showed generally homogeneous FDG uptake of 2.05 ± 0.56 that was comparable to the lung (Table 1). Activity was also seen in the kidneys and in the bladder because FDG is excreted renally (4). While the renal parenchyma showed moderate uptake (Table 1), the urinary collecting system showed marked activity due to the renal concentration process. Hence, intense activity was seen in some patients (Fig. 1A). Spot or linear activity (\geq grade 2) was also seen along the course of the ureter in 5 of the 50 patients.

Other obviously physiological accumulations occurred along the alimentary tract, most notably in the oropharyngeal region (Fig. 3) involving the lingual, sublingual and paralingual areas and extending into the neck region (5). A second alimentary tract structure with FDG accumulation was the intestines (Fig. 4). The appearance of activity in the intestinal tract is variable and exhibits an irregular snake-like course suggesting its presence in intestinal segments. While the highest uptake grade was 3 ($n = 3$), 26 patients exhibited intestinal activity of grade 2, i.e., comparable to the patient's body surface.

Consistent enhancement of around grade 2 and never above 3 was seen in projections to the skin (Figs. 1, 3 and 4). A surface type of activity was also noted along the outer aspects of the liver (Figs. 1A and 5), which, in some instances, was quite marked.

In many ways, the most intriguing accumulation of FDG occurred in various muscle groups. If specific muscular activity was found, the patient was questioned about prior exercise or uncomfortable positioning. The uptake in these regions was variable, as demonstrated in Figure 6. Notable are the large standard deviations in muscular uptake grade, ranging from 1 to 2 (Table 1). While Table 1 is indicative of substantial variations, it is important to exemplify this graphically because the grading scheme cannot capture all variances of muscular uptake.

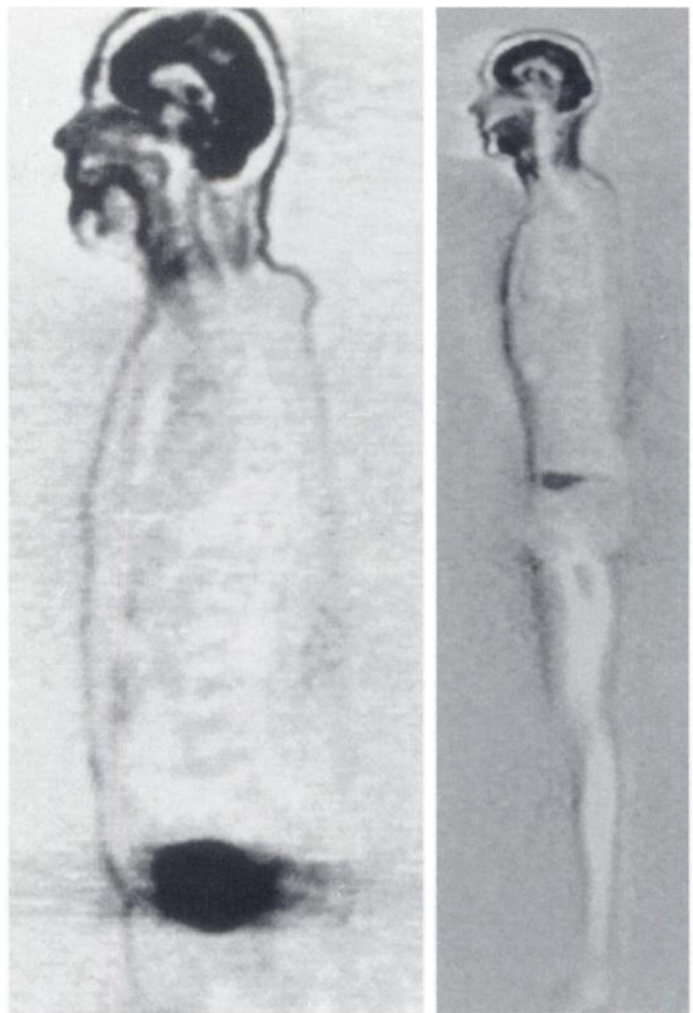


FIGURE 3. Two examples of oropharyngeal activity. (Left) Activity in the buccal area, around the tongue and extending into the pharynx down to the subglottic area. (Right) In another patient, more extensive activity involving the tongue and the anterior neck.

Figures 7A and B show strong uptake in parts of the calf musculature, and activity in the sternocleidomastoid muscle is noted. In another patient (Fig. 7C), substantial uptake is seen in various muscle groups of the proximal upper and lower extremities, while another patient shows marked uptake in all muscle groups of the lower extremities (Fig. 7D). Extensive and notable asymmetric activity is seen in the sternocleidomastoid muscles of a fourth patient (Fig. 7E), while generalized uptake in body musculature was noted on a posterior coronal scan in a fifth patient (Fig. 7F). This patient had been shivering at the time of FDG injection. The patient shown in Figure 7D had taken a vigorous walk over several hundred yards just prior to FDG injection, as he was late for his appointment. The step artifact noted in Figure 7F is a result of the data acquisition protocol which began in the cranial region of the bladder. Only after reaching the head was data acquisition of the lower extremities started.

Upon questioning, we learned that patients with increased muscle activity before or immediately after FDG injection had been uncomfortable. No consistent statements from patients could be elicited that would have explained the cardiac or intestinal activity. Specifically, all patients said that they had fasted prior to scanning.

Physiologic accumulation of FDG led to false-negative diagnosis in three patients with skin metastases of < 3 mm diameter.

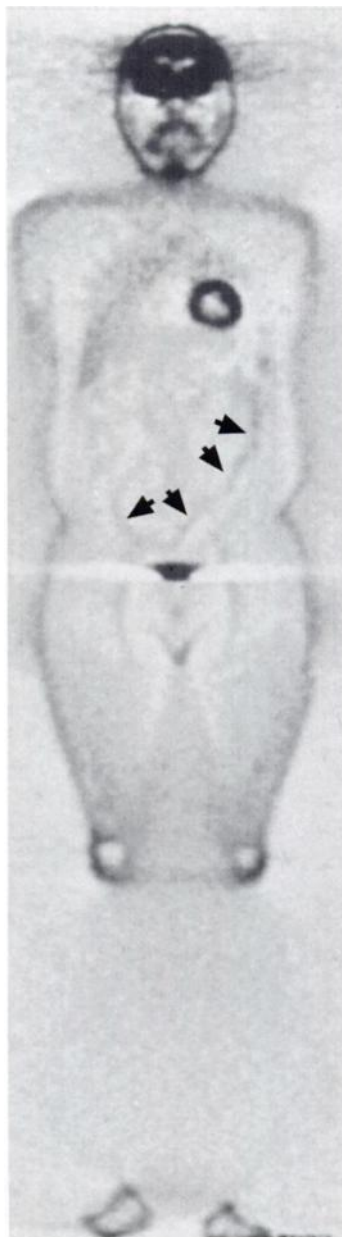


FIGURE 4. Whole-body PET scan shows string-like irregular activity accumulation in the intestinal region (\rightarrow). This patient also shows buccal activity and marked myocardial activity.



FIGURE 5. Increased activity on the outer surface of the liver likely corresponds to a reconstruction artifact in scans not corrected for attenuation.

DISCUSSION

So far, most PET examinations have been used to evaluate a circumscribed body area when looking for malignant disease, which emphasizes quantitative measurements requiring absorption correction and region of interest (ROI) data analysis. The advent of whole-body PET scanners allows whole-body emission scanning in approximately 1 hr. Therefore, a different imaging strategy can be considered. Since whole-body attenuation correction is too time-consuming (15), we focused on evaluating nonattenuation-corrected whole-body scans. When evaluating these scans for malignant tissue, we have found that reading the coronal and sagittal images offer the best means of image analysis. Hence, in the study presented here, we were mainly interested in defining normal nonattenuation corrected scan appearance in the coronal and sagittal planes.

Interpretation of these whole-body FDG-PET images requires experience with normal variations in scans that could cover or mimic disease. It is therefore important to identify normal FDG accumulations on such scans. Two types of normal activities were observed and can be classified as technical/artifactual and physiological.

Artifactual enhancement of surface structures in scans not corrected for attenuation is noted consistently on the body surface mimicking increased accumulation in the skin (Fig. 1B) and at the surface of other structures which show some FDG accumulation such as the liver (Fig. 5). The recognition of these artifacts is important, but because of their rim-like appearance it is unlikely that they are misinterpreted with pathology; pathology typically presents as focal increase of FDG accumulation. Furthermore, a cutaneous lesion in a patient with

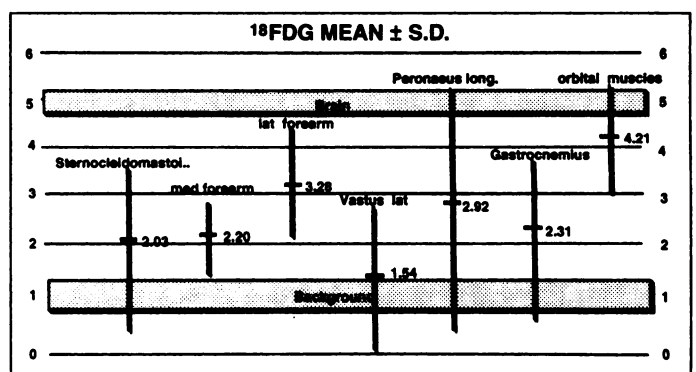


FIGURE 6. Mean and s.d. for activity in various muscle groups.

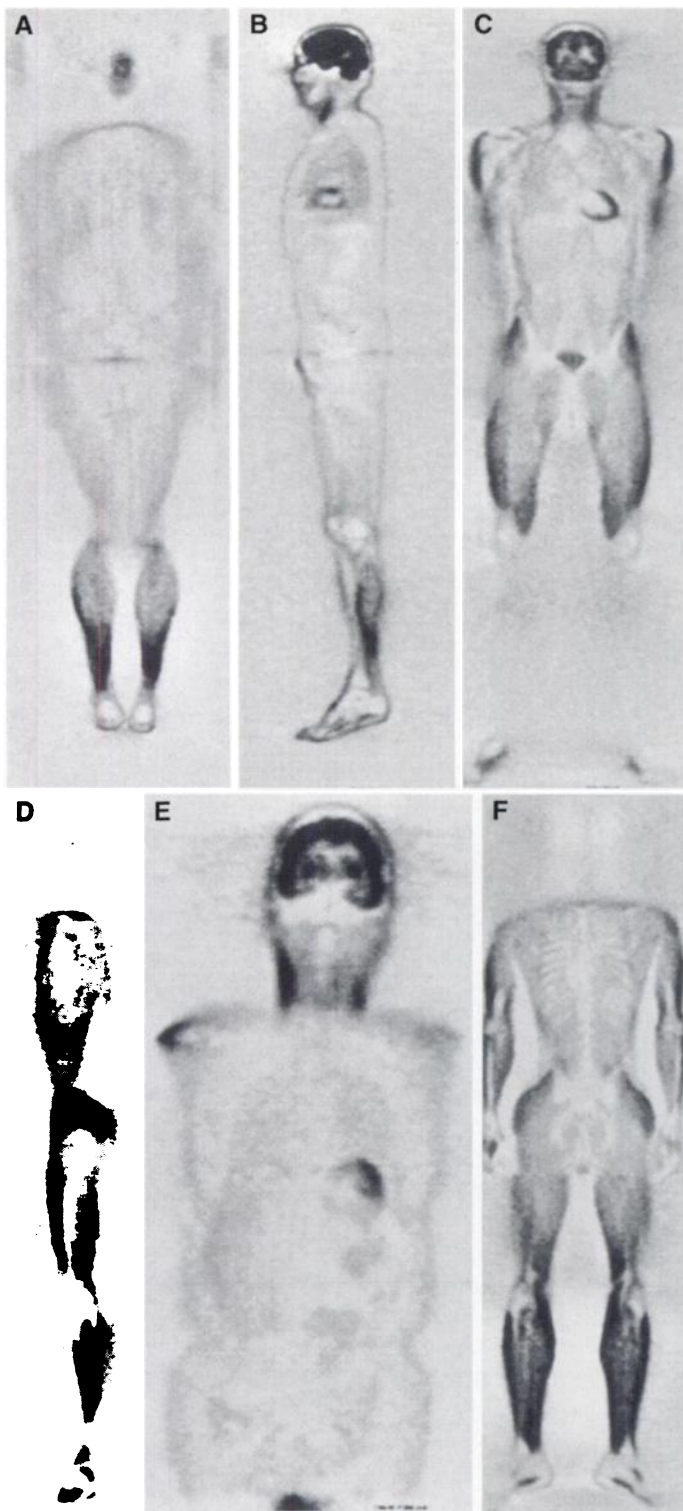


FIGURE 7. (A) and (B) differential uptake into the calf muscles. (C) Uptake into proximal muscle groups of upper and lower extremities, and (D) the entire musculature of the lower left extremity. (E) Asymmetric uptake into the sternocleidomastoid. (F) Diffusely increased uptake throughout the body musculature.

cutaneous melanoma would show proportionately increased activity relative to the skin in an uncorrected scan and still be clearly distinguishable from its surroundings.

In the unlikely case where surface enhancement artifacts pose a problem, and this is recognized right after image reconstruction, the patient can be rescanned in the area of interest, because new software developments permit transmission scans to be

acquired in the presence of emission (16). In a particular body ROI, an absorption-corrected image stack can be obtained. Some of the images, such as Figures 1B, 3A and 3B, show increased surface accumulation in the peribuccal area. Whether this activity is simply surface enhancement due to buccal musculature motion or active saliva cannot be answered definitively. Yet, this type of activity is usually not interpreted as a pathologic lesion.

Physiological FDG accumulations of variable intensity occur in many organs because they metabolize glucose. The strong accumulation of FDG in the brain, and in the renal calices and bladder where FDG is excreted, is well known. Other organs exhibiting consistent, albeit weaker, accumulation are the liver, renal parenchyma and the bone marrow. There is also inconsistent but homogenous accumulation in the breast and inhomogenous accumulation in the intestines. The accumulation in these organs must be recognized and it is conceivable that moderate liver or lung uptake may obscure a pathological lesion. Renal caliceal and ureteral spot activities may be a problem. While transaxial section evaluation or superimposition of PET scans on cross-sectional morphologic image data will usually permit clear determination whether activity accumulation is within or just outside the kidney, spot activity in the ureters could be easily viewed as a pathological lymph node. Here, rescanning of the patient in the critical region will usually help because the site of ureteral activity will vary. A second potential problem area for proper image interpretation is the intestines, where inhomogeneity of uptake can mimic small tumorous lesions with relatively weak FDG uptake. There are no fool-proof remedies against misinterpretation of intestinal accumulation. If a whole-body scan is available, it may be easier to delineate the activity.

FDG accumulation in striated muscle is a well-known phenomenon, but only during whole-body scanning does the extent of such accumulations become apparent. Our data suggest that most increased accumulations are related to physical activity of that particular muscle group in the time before and immediately after injection. With the proper measures, it should be possible to minimize such uptake, thereby enhancing lesion detectability. Patients should be told to avoid vigorous physical activity prior to FDG injection.

Just as important, is that the patient should be as comfortable and relaxed as possible with much support in a recumbent position during and after injection. This will prevent involuntary tensing of muscle groups such as the neck muscles or the muscles of the upper extremity. Particularly when scanning for metastatic lymph nodes in the neck, there should be minimal muscular activity in this area. This is also necessary for the buccal region, where frequently seen activity can be associated with saliva, the tonsils or muscular activity related to swallowing or talking. While saliva can be rinsed away prior to scanning and the patient can be asked not to talk while waiting for the scan, activity due to swallowing and in the tonsils will remain.

The ocular musculature also has very high activity and will be difficult to rest. Finally, the heart muscle showed uptake in a substantial number of patients despite their 4-hr fast prior to scanning. Apparently, there are many patients in whom glucose consumption of the heart continues in the fasted state and is not replaced by free fatty acid metabolism. Cardiac activity is, however, only a problem when dealing with metastatic pulmonary disease or in the cardio-phrenic angle. Although the coronal and sagittal cross-sections are best used for tumor staging, transaxial scans are helpful whenever accumulation is present that could be related to muscular activity.

CONCLUSION

Most physiological activity in FDG whole-body PET scans for tumor staging is visualized consistently. The brain, lung, liver, bone marrow and urinary system are consistently seen. Cardiac activity is inconsistent and related to the switch from FDG to free fatty acid metabolism (12). The most striking and irregular FDG uptake pattern is associated with various muscle groups that are exercised just before FDG injection. Because "hot" muscle groups can interfere with the diagnostic quality of a scan, care should be taken, particularly in the neck region, to rest the patient comfortably before injection. Lastly, knowing the muscle groups that have strong FDG accumulation will be extremely helpful in differentiating activity from pathological lesions.

REFERENCES

1. Som P, Atkins HL, Bandyopadhyay D, et al. A fluorinated glucose analog, 2-fluoro-2-deoxy-D-glucose (F-18): nontoxic tracer for rapid tumor detection. *J Nucl Med* 1980;21:670-675.
2. Strauss LG, Conti PS. The applications of PET in clinical oncology. *J Nucl Med* 1991;32:623-648.
3. Hawkins RA, Hoh CK, Glaspy JA, et al. The role of positron emission tomography in oncology and other whole-body applications. *Semin Nucl Med* 1992;22:268-284.
4. Hoh CK, Hawkins RA, Glaspy JA, et al. Cancer detection with whole-body PET using 2-[¹⁸F]fluoro-2-deoxy-D-glucose. *J Comput Assist Tomogr* 1993;17:582-589.
5. Jabour B, Choi Y, Hoh CK, et al. Extracranial head and neck PET imaging with 2-[¹⁸F] fluoro-2-deoxy-D-glucose and MR imaging correlation. *Radiology* 1993;186:27-35.
6. Wahl RL, Helvie MA, Chang AE, Andersson I. Detection of breast cancer in women after augmentation mammoplasty using fluorine-18-fluorodeoxyglucose-PET. *J Nucl Med* 1994;35:872-875.
7. Newmann JS, Francis IR, Kaminski MS, Wahl RL. Imaging of lymphoma with PET with 2-[¹⁸F]-fluoro-2-deoxy-D-glucose: correlation with CT. *Radiology* 1994;190:111-116.
8. Wahl RL, Quint LE, Greenough RL, Meyer CR, White RI, Orringer MB. Staging of mediastinal non-small cell lung cancer with FDG PET, CT, and fusion images: preliminary prospective evaluation. *Radiology* 1994;191:371-377.
9. Tyler J, Strother S, Zatorre R, et al. Stability of regional cerebral glucose metabolism in the normal brain measured by positron emission tomography. *J Nucl Med* 1988;29:631-642.
10. Maquet P, Dive D, Salmon E, von Frenckel R, Franck G. Reproducibility of cerebral glucose utilization measured by PET and the [¹⁸F]-2-fluoro-2-deoxy-D-glucose method in resting, healthy human subjects. *Eur J Nucl Med* 1990;16:267-273.
11. Schwaiger M, Hicks R. The clinical role of metabolic imaging of the heart by positron emission tomography. *J Nucl Med* 1991;32:565-578.
12. Choi Y, Brunken R, Hawkins RA, et al. Factors affecting myocardial 2-[¹⁸F]-fluoro-2-deoxy-D glucose uptake in positron emission tomography studies of normal humans. *Eur J Nucl Med* 1993;20:308-318.
13. Voipio-Pulkki LM, Nuutila P, Knutti MJ, et al. Heart and skeletal muscle glucose disposal in type 2 diabetic patients as determined by positron emission tomography. *J Nucl Med* 1993;34:2064-2067.
14. Hamacher K, Coenen HH, Stoecklin G. Efficient stereospecific synthesis of no-carrier-added 2-[¹⁸F]-fluoro-2-deoxy-D glucose using ammoniumpolyether supported nucleophilic substitution. *J Nucl Med* 1986;27:235-238.
15. Dahlbom M, Hoffman EJ, Hoh CK, et al. Whole-body positron emission tomography: Part I. Methods and performance characteristics. *J Nucl Med* 1992;33:1191-1199.
16. Oda K, Senda M, Toyama H, Ishii K, Amano M. Attenuation correction using postinjection transmission measurements for PET: the optimization of measurement conditions. *Kaku Igaku* 1994;31:37-41.

Thyroglobulin Determination, Neck Ultrasonography and Iodine-131 Whole-Body Scintigraphy in Differentiated Thyroid Carcinoma

Maja Franceschi, Zvonko Kusić, Dinko Franceschi, Ljerka Lukinac and Sanja Rončević

Department of Nuclear Medicine and Oncology, University Hospital, Sestre Milosrdnice, Zagreb, Croatia; and Department of Radiology, SUNY, Stony Brook, New York

The long-term prognosis of patients with differentiated thyroid carcinoma depends on the early diagnosis and treatment of metastases and local recurrences. We evaluated serum thyroglobulin measurements, neck ultrasonography with ultrasound-guided biopsy and ¹³¹I whole-body scintigraphy in the follow-up of 359 patients after surgical thyroidectomy and radioiodine ablation of the thyroid remnant. **Methods:** Serum thyroglobulin levels were determined and considered abnormal when the values were >5 ng/ml. Ultrasonography over the entire neck region and fine-needle aspiration biopsy of the mass or enlarged lymph nodes were carried out using 5- and 7.5-MHz transducers and 23-gauge needles. Whole-body scintigraphy was performed after administration of 185 MBq (5 mCi) ¹³¹I. **Results:** Increased levels of thyroglobulin (ranging from 12 to >600 ng/ml) were measured in 40 of 55 (73%) patients with metastases or local recurrences. Ultrasonography revealed occult neck masses that were not detected by other methods. Neck ultrasonography and ultrasound-guided biopsy were positive for malignancy in 23 patients. Thyroglobulin levels were undetectable in 12 (52%) of these patients and ¹³¹I whole-body scintigraphy was negative in 19 (83%) of them. **Conclusion:** The combined use of three diagnostic modalities (measurement of serum thyroglobulin, neck ultrasonography with ultrasound-guided biopsy for detecting

recurrences of carcinoma in the neck region and ¹³¹I whole-body scintigraphy) appears to give the best results in the follow-up of patients with differentiated thyroid carcinoma.

Key Words: thyroid carcinoma; thyroglobulin; neck ultrasonography; iodine-131; whole-body scintigraphy

J Nucl Med 1996; 37:446-451

Iodine-131 whole-body scintigraphy and serum thyroglobulin measurements are considered to be the most effective methods in the follow-up of patients with differentiated thyroid carcinoma who have undergone surgical thyroidectomy and radioiodine ablation of the thyroid remnant. Both diagnostic procedures, however, have some disadvantages. The major drawback of ¹³¹I whole-body scintigraphy is the necessity to withdraw thyroid hormone suppression therapy, with the subsequent onset of hypothyroidism and its physical and psychological effects (1). Also, highly specific radioiodine scintigraphy may give false-negative results (2).

Numerous studies have shown that the determination of serum thyroglobulin levels is a suitable procedure for the follow-up of patients with thyroid carcinoma (3-9). The method's most important advantage is the detection of metastases or recurrences in patients who are on thyroid suppression therapy. It is still, however, controversial whether thyroid hormone

Received Feb. 2, 1995; revision accepted Jun. 29, 1995.

For correspondence or reprints contact: Maja Franceschi, MD, PhD, Department of Nuclear Medicine and Oncology, University Hospital "Sestre Milosrdnice," Vinogradska 29, 41000 Zagreb, Croatia.